ORIGINAL RESEARCH

HIF-1α, TWIST-1 and ITGB-1, associated with Tumor Stiffness, as Novel Predictive Markers for the Pathological Response to Neoadjuvant Chemotherapy in Breast Cancer

Jing Zhang[1]
Shuo Zhang[2]
Song Gao[3]
Yan Ma[1]
Xueying Tan[1]
Ye Kang [4]
Weidong Ren [1]

[1]Department of Ultrasound, Shengjing Hospital of China Medical University, Shenyang, Liaoning 110004, People's Republic of China; [2]Department of Neurology, Shengjing Hospital of China Medical University, Shenyang, Liaoning 110004, People's Republic of China; [3]Department of Clinical Oncology, Shengjing Hospital of China Medical University, Shenyang, Liaoning 110004, People's Republic of China; [4]Department of Pathology, Shengjing Hospital of China Medical University, Shenyang, Liaoning 110004, People's Republic of China

Purpose: To investigate the relationship between hypoxia-inducible factor 1-alpha (HIF-1α), Twist family BHLH transcription factor 1 (TWIST-1), and β1 integrin (ITGB-1) expression and tumor stiffness, and evaluate performance of HIF-1α, TWIST-1, and ITGB-1 alone and in combination with Ki-67 for predicting pathological responses to neoadjuvant chemotherapy (NACT) in breast cancer (BC).

Patients and Methods: This was a prospective cohort study of 104 BC patients receiving NACT. Tumor stiffness and oxygen score (OS) were evaluated before NACT by shear-wave elastography and optical imaging; HIF-1α, TWIST-1, ITGB-1, and Ki-67 expression were quantitatively assessed by immunohistochemistry of paraffin-embedded tumor samples obtained by core needle biopsy. Indexes were compared among different residual cancer burden (RCB) groups, and associations of HIF-1α, TWIST-1, ITGB-1, and Ki-67 with tumor stiffness and OS were examined. The value of HIF-1α, TWIST-1, ITGB-1, and Ki-67, and a possible new combined index (predRCB) for predicting NACT responses was assessed by receiver operating characteristic (ROC) curves.

Results: HIF-1α, TWIST-1, and ITGB-1 expression were positively correlated with tumor stiffness and negatively with OS. Area under the ROC curves (AUCs) measuring the performance of HIF-1α, TWIST-1, ITGB-1, and Ki-67 for predicting responses to NACT were 0.81, 0.85, 0.79, and 0.80 for favorable responses, and 0.83, 0.86, 0.84, and 0.85 for resistant responses, respectively. PredRCB showed better prediction than the other individual indexes for favorable responses (AUC = 0.88) and resistant responses (AUC = 0.92).

Conclusion: HIF-1α, TWIST-1, ITGB-1, and Ki-67 performed well in predicting favorable responses and resistance to NACT, and predRCB improved the predictive power of the individual indexes. These results support individualized treatment of BC patients receiving NACT.

Keywords: HIF-1α, TWIST-1, ITGB-1, neoadjuvant chemotherapy, breast cancer, prediction

Introduction

Neoadjuvant chemotherapy (NACT) plays an indispensable role in the treatment of breast cancer (BC). Pathological complete response (PCR) is used as a surrogate prognostic marker for long-term disease-free survival after NACT in BC.[1,2] Approximately 30% of cancers achieve PCR after NACT.[3] However, certain risk factors are associated with the development of chemotherapy resistance.[4] Moreover,

Correspondence: Weidong Ren
Department of Ultrasound, Shengjing Hospital of China Medical University, No. 36, Sanhao Street, Heping District, Shenyang City 110004, People's Republic of China
Email renwdcmu01@163.com

because BC can progress during NACT, determining the optimal time for surgical intervention is difficult. Therefore, early prediction of the pathological response to NACT is critical, and it may help optimize individual chemotherapeutic strategies in BC patients.

Among the established clinicopathological markers, only Ki-67, estrogen receptor (ER), and human epidermal growth factor receptor 2 (HER2) have shown clear clinical applicability,[4,5] and of these, only Ki-67 was reported to be an accurate biomarker for predicting PCR to NACT.[6] However, the predictive efficacy of a single biomarker remains controversial. Gene expression analysis may improve our understanding of the biological behavior of BC, and although some genes may be useful indicators for the early identification of NACT responses,[7,8] the high costs associated with their analysis limit their routine clinical application. Therefore, the identification of an effective biomarker to predict NACT responses and optimize the treatment of BC is an urgent need.

It is reported that BC with high matrix stiffness evaluated by pre-treatment ultrasound elastography is strongly correlated with chemoresistance.[9,10] Tumor stiffness is largely determined by the collagen composition of the extracellular matrix (ECM), which has profound effects on BC progression, invasion, metastasis, and chemoresistance.[11] Recent studies show that high matrix stiffness could induce epithelial to mesenchymal transition (EMT) and tumor progression by activating Twist family BHLH transcription factor 1 (TWIST-1).[12,13] In addition, TWIST-1 overexpression is associated with short survival and a poor response to chemotherapy in patients with cancer.[2,14,15]

Hypoxia-inducible factor 1-alpha (HIF-1α), which mediates adaptation to hypoxia in cells, has been shown to be associated with matrix stiffness.[16] Activation of the hypoxia pathway by HIF-1α contributes to the development of radiotherapy and chemotherapy resistance.[17] HIF-1α can also directly upregulate TWIST-1 expression.[18,19]

Integrins play an important role in maintaining mammary stem cells in the normal breast. Dysregulation of integrin signaling distorts cell–cell or cell–ECM interactions and promotes BC progression by inducing chemoresistance and metastasis.[20,21] A recent study showed that β1 integrin (ITGB-1) plays a pivotal role in the regulation of matrix stiffness,[22] and ITGB-1 expression is associated with chemoresistance and metastasis in BC.[20,21]

Most of the studies cited above were based on basic experiments in vitro or in animal models. However, no study has investigated the relationships between HIF-1α,

TWIST-1, and ITGB-1 expression and tumor stiffness in BC patients, or the predictive diagnostic performance of these biomarkers for predicting NACT responses. Here, we analyzed 104 patients who received NACT to determine the association of HIF-1α, TWIST-1, and ITGB-1 expression with tissue stiffness, oxygen score (OS), and pathological responses. In addition, we investigated the power of HIF-1α, TWIST-1, and ITGB-1 alone or in combination with Ki-67 to predict the response to NACT in BC.

Materials and Methods
Patients
A total of 112 women were enrolled between February 2014 and July 2019. All patients were diagnosed with invasive BC by ultrasound-guided core needle biopsy (CNB) and received NACT and subsequent surgical intervention. Eight patients were excluded because of changes in the treatment regimen or other unspecified reasons. The study was conducted with the approval of the ethics committee of Shengjing Hospital of China Medical University. All patients provided written informed consent.

Chemotherapy Regimen
Prior to surgery, all patients (n = 104) had received six cycles of NACT. The detailed chemotherapy regimens are as follows: 66 received TEC (docetaxel, epirubicin, and cyclophosphamide); 11 received TE (docetaxel and epirubicin); 9 received FEC (5-fluorouracil, epirubicin, and cyclophosphamide); and 18 classified as HER2+ received the targeted drug herceptin (trastuzumab) in addition to the docetaxel-based regimen.

Shear-Wave Elastography (SWE) Stiffness Evaluation
Tumor stiffness was evaluated using an ultrasound diagnostic imaging system, Aixplorer (SuperSonic Imagine, Aix en Provence, France), with a 4–15 MHz linear transducer. Four SWE images were obtained on two orthogonal planes for each lesion without outside pressure. Gray-scale and SWE images were simultaneously displayed in the split-screen mode. Tissue elasticity was assessed according to a color-coded map, with colors ranging from blue (soft) to red (hard). An optionally sized region of interest (ROI) trace (Q-box trace; SuperSonic Imagine) was drawn to include the lesion and peritumoral stroma. Then, quantitative elasticity values representing the Young modulus in kilopascals

(range: 0–300 kpa) were automatically calculated and presented by the SWE system. Finally, the maximum elasticity (Emax) and mean elasticity (Emean) values of a lesion were recorded, and the average results of the four images were used for further analysis.

Breast Relative Oxygen Saturation Evaluation

The OS of the tumors was evaluated using the dynamic optical breast imaging (DOBI) system, TM-A02 (TRKM Medical Technology Co., Ltd, Shenzhen, China), which is equipped with a high-intensity probe (with a dual-wavelength LED illuminator at 730 and 850 nm) and a near-infrared camera (resolution: 570–600 lines; sensitivity: 0.001–0.01 Lux). The probe emits red light, which penetrates breast tissues and shows a different absorption or scatter pattern when meeting a neoangiogenic area compared with that in other tissues. This is attributed to differences in the distribution of oxygenated and deoxygenated hemoglobin.[23]

OS evaluation was performed in the dark. The patients exposed their upper body and sat facing the machine at a distance of 55–75 cm. First, the examiner palpated the five breast quadrants and the axillary area bilaterally. The probe was placed under the breast to be examined (outer or lower quadrant). The examiner adjusted the sharpness and brightness of the image to ensure that the entire breast was captured and that the vasculature in the breast tissue was clearly displayed. For each image, the probe was retained for at least 2 seconds to complete the acquisition. The system then generated a two-dimensional distribution image and a functional image. The relative oxygen content distribution of the area was represented by a color-coded map on the functional image (with colors ranging from green to red). Then, the ROIs were selected, and the system automatically calculated the OS of the lesion. OS represents the relative oxygen saturation of the ROI.[23]

Tumor SWE stiffness and the OS of all patients were evaluated one day before NACT.

Immunohistochemistry and Pathology

Pathologic assessments were conducted in two steps.

First, samples from ultrasound-guided CNBs were examined to confirm the histopathological characteristics and molecular subtypes of the tumors.

Immunohistochemistry

Anti-ER (Clone SP1, Roche, USA), anti-PR (Clone 1E2, Roche, USA), and anti-HER2 antibodies (Clone 4B5, Roche, USA), anti-HIF-1α (dilution 1:250; Clone EPR3658, Abcam, USA), anti-TWIST-1 (dilution 1:200; Clone 10E4E6, Abcam, USA), anti-ITGB-1 (dilution 1:200; Clone EPR1040Y, Abcam, USA), and anti-Ki-67 antibodies (dilution 1:200; Clone SP6, Abcam, USA) were used for immunohistochemical staining. Immunohistochemistry procedures were performed according to the manufacturers' instructions.

Immunohistochemical Evaluation

Positive staining for ER and PR was defined as nuclear staining in ≥1% of the tumor cells. HER2 was assessed based on the intensity of tumor cell membrane staining; HER2-positivity was indicated by a 3+ or 2+ score and was confirmed by fluorescence in situ hybridization (FISH).[24]

HIF-1α, TWIST-1, ITGB-1, and Ki-67 expression levels were scored by two independent clinical doctors who had no prior knowledge of the prognosis or other clinicopathological variables, using a weighted Histoscore method, also known as the H-score.[25] Briefly, the percentage of positive cells per slide (0% to 100%), as the average of ten random fields (400x, diameter: 0.55mm) screened, and the dominant intensity pattern of staining (0, absent; 1, weak; 2, moderate; 3, intense) were measured for each tumor section. H-scores for each sample were determined by multiplying the staining intensity by the percentage of positive cells (range, 0 to 300). Positivity for HIF-1α and TWIST-1 was defined as positive nuclear and cytoplasmic staining. Positivity for ITGB-1 was defined as positive membrane and cytoplasmic staining. Positivity for Ki-67 was defined as positive nuclear staining.

According to the St. Gallen International Expert Panel consensus,[26] all lesions were classified into four major molecular subtypes: luminal A, luminal B, triple negative, and HER2-positive.

Second, all surgical specimens were collected to assess NACT responses. We opted for the web-based MD Anderson Residual Cancer Burden (RCB) calculator (http://www3.mdanderson.org/app/medcalc/index.cfm?pagename=jsconvert3).

This method allows calculation of an index that combines pathology measurements of the primary tumor (size and cellularity) and nodal metastases (number and size) as follows: $RCB = 1.4\ (f_{inv}d_{prim})^{0.17} + [4(1-0.75^{LN})\ d_{met}]^{0.17},$[27]

where f_{inv} is the proportion of primary tumor area containing invasive carcinoma; d_{prim} is the bidimensional diameters of the primary tumor bed; LN is the number of positive lymph nodes; and d_{met} is the diameter of the largest nodal metastasis. Using two cut-off points, four RCB categories were proposed as follows: RCB-0 (PCR, RCB = 0), RCB-I (RCB = 0−1.36), RCB-II (RCB = 1.36−3.28), and RCB-III (RCB > 3.28).[27] Favorable responses to NACT were classified as RCB-0 or RCB-I, whereas RCB-III represented resistance to NACT (pathological non-responders). Pathologic assessments for all lesions were performed according to the World Health Organization classification standards.

Statistical Analysis

Statistical analyses were performed using SPSS 23.0 software (IBM, USA), GraphPad Prism version 5.0 (GraphPad Software, USA), and Sigmaplot version 14.0 (Systat Software, USA). Continuous variables with normal distribution were expressed as the mean ± standard deviation, skewed distributions were expressed as the median and interquartile range, and categorical variables were expressed as counts and percentages. Comparisons among three groups (PCR+RCB-I, RCB-II, and RCB-III) were performed using the χ^2 test, Kruskal–Wallis test or analysis of variance (ANOVA). *Post hoc* analysis was used for pairwise comparisons among three groups if the results of the Kruskal–Wallis test or ANOVA test were significant. *Bonferroni method* analysis was also performed for pairwise comparisons among three groups if the results of the χ^2 test were significant. Inter-observer reproducibility of Ki-67, HIF-1α, TWIST-1, and ITGB-1 was assessed by computing intra-class correlation coefficients (ICC). The detail parameters were as follows: Model: Two-Way Mixed-Effect model; Type: single measure; Definition: absolute agreement.[28] Pearson's correlation (rp) and Spearman's correlation (rs) analyses were used to analyze the relationships among SWE stiffness, OS, HIF-1α, TWIST-1, and ITGB-1 expression. The area under the ROC curve (AUC) values were used to determine the predictive diagnostic performance of HIF-1α, TWIST-1, ITGB-1, and Ki-67. A new predictive biomarker (predRCB) was combined with the largest AUC of new predictors (HIF-1α, TWIST-1, and ITGB-1) and the traditional one (Ki-67) according to the results of the multivariable linear regression model. Differences were considered significant when the two-sided *P* value was <0.05.

Results

Baseline Characteristics of Patients in the Three Groups

The baseline characteristics are summarized in Table 1. Among the 104 patients who underwent breast and axillary surgery 3–4 weeks after NACT, 23 (22%) showed a favorable response (PCR and RCB-I), 48 (46.2%) showed a moderate response (RCB-II), and 33 (31.7%) showed NACT resistance (RCB-III). In the subpopulations according to molecular subtype, the rate of PCR+RCB-I was 21.7% in the triple negative type, 26.1% in the HER2-positive type, 17.4% in the luminal A type, and 39.1% in the luminal B type. The RCB-III rate was 0% in the triple negative type, 4.2% in the HER2-positive type, 21.2% in the luminal A type, and 72.7% in the luminal B type. There were significant differences among the three RCB groups ($P < 0.05$) for most clinical indicators, except for HER2 positivity in "Immunohistochemical marker", T2 in "Tumor size", Grade 2 and Grade 3 in "Grade", and IIIB in "Clinical stage". The imaging indicators Emax, Emean, and OS were also significantly different among the three groups ($P < 0.05$). Figures 1 and 2 show the SWE and DOBI images of one lesion 1 day before NACT, respectively.

HIF-1α, TWIST-1, ITGB-1, and Ki-67 Expression in the Three Groups

The expression of HIF-1α, TWIST-1, ITGB-1, and Ki-67 was detected in 104 preoperative tumor biopsy specimens (Figure 3A–H). Inter-observer reliability was good, with ICC values of 0.839 (0.771–0.888), 0.837 (0.769–0.886), 0.877 (0.823–0.915), and 0.804 (0.723–0.863) for Ki-67, HIF-1α, TWIST-1, and ITGB-1, respectively. The expression levels of HIF-1α, TWIST-1, ITGB-1, and Ki-67 in the different RCB groups are presented in Table 2. The expression of all biomarkers differed significantly among the three RCB groups ($P < 0.01$). Specifically, patients in the resistance group showed higher HIF-1α, TWIST-1, and ITGB-1 expression and lower Ki-67 expression, whereas those in the favorable response group showed lower HIF-1α, TWIST-1, and ITGB-1 expression and higher Ki-67 expression.

Correlations Between SWE Stiffness, OS, HIF-1α, TWIST-1, ITGB-1, and Ki-67 Expression

Correlation analysis revealed negative correlations between Emax and OS *(rs = –0.812, P < 0.001)* and

Table 1 Baseline Characteristics of Patients

Characteristic	Total	PCR+RCB-I	RCB-II	RCB-III	P value
RCB scores	2.1 (1.5–3.6)	0 (0–1.2)	2.1 (1.8–2.7)	4.0±0.5	<0.001[#,a,b,c]
Patients number	104	23	48	33	
Age (years)	49.0 (38.0–57.0)	46.0 (43.0–53.0)	49.0 (32.0–57.0)	50.2±11.1	0.187[#]
Largest diameter (cm)	4.0 (2.3–5.0)	4.0(2.0–6.0)	3.0 (2.3–4.0)	4.0 (3.0–6.0)	0.192[#]
Immunohistochemical marker					
Ki-67 (%)	32.5±18.9	50.0±21.3	33.7±14.9	18.6±9.4	<0.001[¥,a,b,c]
ER positive, n (%)	62	12 (52.2)	20 (41.7)	30 (90.1)	<0.001[*,b,c]
PR positive, n (%)	56	8 (34.8)	20 (41.7)	28 (84.8)	<0.001[*,b,c]
HER2 positive, n (%)	35	7 (30.4)	20 (41.7)	8 (24.2)	0.247[*]
Molecular subtype, n (%)					
Luminal A	13	4 (17.4)	2 (4.2)	7 (21.2)	0.039[*,c]
Luminal B	51	9 (39.1)	18 (41.8)	24 (72.7)	0.004[*,b,c]
Triple negative	20	5 (21.7)	15 (31.2)	0 (0)	<0.001[*,b,c]
HER2 positive	20	6 (26.1)	13 (27.1)	2 (4.2)	0.032[*]
Pathological types, n (%)					
Invasive ductal carcinoma	95	19 (82.6)	47 (97.9)	29 (87.9)	0.04[*]
Invasive lobular carcinoma	9	4 (17.4)	1 (2.1)	4 (12.1)	0.04[*]
Tumor size (cT), n (%)					
T1	9	2 (8.7)	7 (14.6)	0 (0)	0.047[*]
T2	72	13 (56.5)	36 (75.0)	23 (69.7)	0.297[*]
T3	23	8 (34.7)	5 (10.4)	10 (30.3)	0.022[*,a]
Grade, n (%)					
Grade 2	90	19 (82.6)	43 (89.6)	28 (84.8)	0.662[*]
Grade 3	14	4 (17.4)	5 (10.4)	5 (15.1)	0.662[*]
Clinical stage					
IIA	12(11.5)	7 (30.4)	5 (10.1)	0 (0)	0.001[*,b]
IIB	40(38.5)	6 (26.1)	27(56.2)	7 (21.2)	0.002[*,c]
IIIA	45(43.3)	8 (34.8)	16 (33.3)	21 (63.6)	0.002[*,c]
IIIB	4(3.8)	2 (8.7)	0 (0)	2 (6.1)	0.098[*]
IIIC	3(2.9)	0 (0)	0 (0)	3 (9.1)	0.040[*]
SWE stiffness					
Emax	147.9±65.5	114.7±34.9	141.2±56.9	180.7±78.9	0.001[¥,a,b]
Emean	49.0±24.3	41.5±13.2	44.7±21.1	60.4±30.3	0.003[¥,b,c]
OS	0.3 (0.2–0.5)	0.6±0.2	0.2 (0.2–0.4)	0.3±0.2	<0.001[#,a,b]

Notes: [*]χ^2 test; [#]Kruskal–Wallis test; [¥]ANOVA test; [a]significant difference for pairwise comparison between PCR+RCBI and RCBII; [b]significant difference for pairwise comparison between PCR+RCBI and RCBIII; [c]significant difference for pairwise comparison between RCBII and RCBIII.
Abbreviations: PCR, pathological complete response; RCB, residual cancer burden; ER, estrogen receptor; PR, progesterone receptor; HER2, human epidermal growth factor receptor 2; Emax, maximum elasticity; Emean, mean elasticity; OS, oxygen score; SWE, shear-wave elastography; n (%), number (%).

Emean and OS $(rs = -0.715, P < 0.001)$; positive correlations were observed between HIF-1α and TWIST-1 expression $(rs = 0.797, P < 0.001)$, between HIF-1α and ITGB-1 expression $(rp = 0.852, P < 0.001)$, and between TWIST-1 and ITGB-1 expression $(rs = 0.814, P < 0.001)$; negative correlations were observed between Ki-67 and HIF-1α expression $(rp = -0.404, P < 0.001)$, between Ki-67 and TWIST-1 expression $(rs = -0.467, P < 0.001)$, and between Ki-67 and ITGB-1 expression $(rp = -0.358, P < 0.001)$. The correlations of immunohistochemical features with SWE stiffness and OS at baseline are shown in Table 3. The results showed that HIF-1α, TWIST-1, and ITGB-1 expression levels were positively correlated with SWE stiffness (Emean and Emax) and negatively correlated with OS. In addition, Ki-67 showed no or weak correlation with SWE stiffness and OS at baseline.
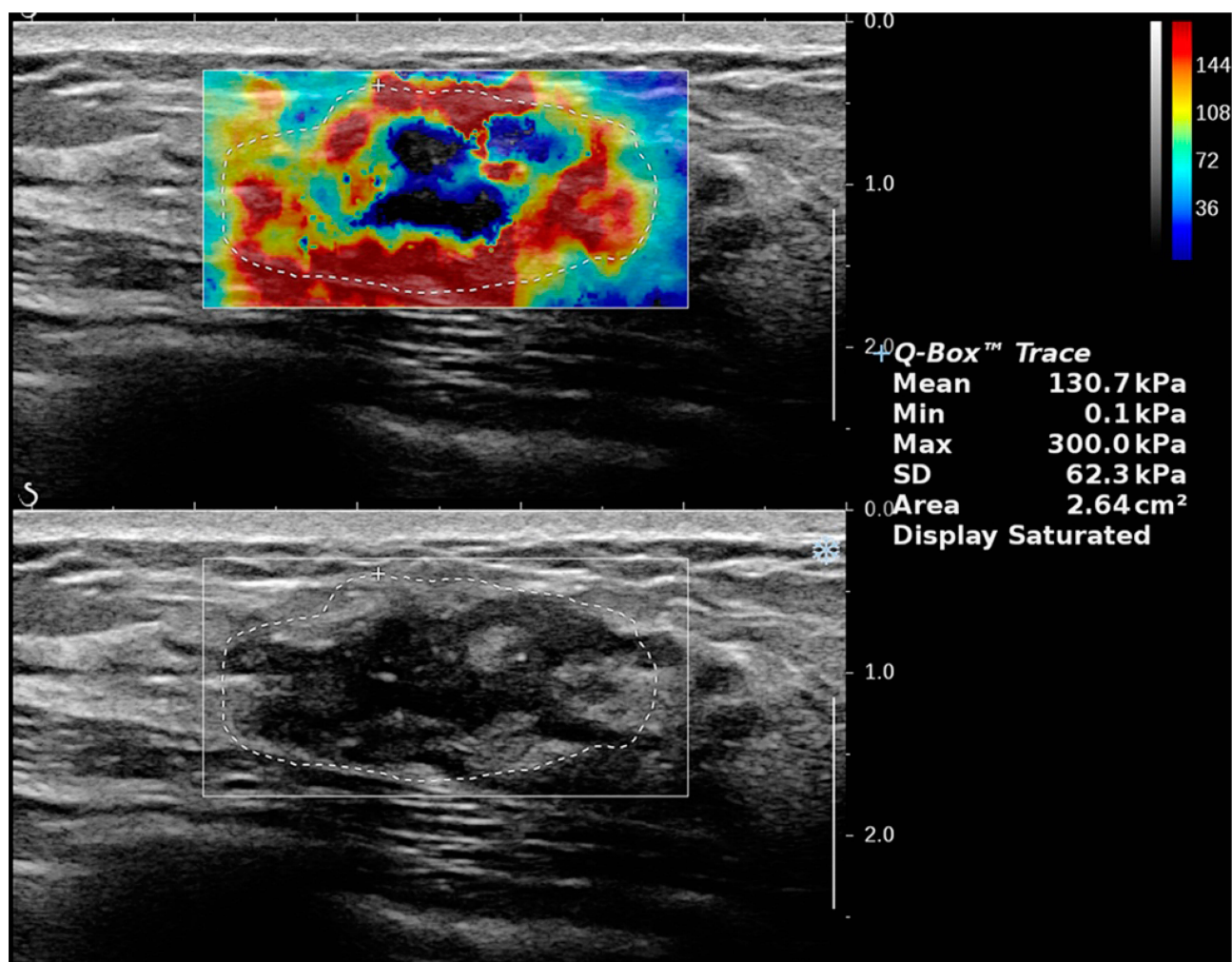
Figure 1 SWE image with a ROI placed over the stiffest part of the lesion with the Emax and Emean values being automatically calculated by the system.
Abbreviations: Emax, maximum elasticity; Emean, mean elasticity; ROI, region of interest; SWE, shear-wave elastography.

Performance of HIF-1α, TWIST-1, ITGB-1, Ki-67, and PredRCB for Predicting the Response to NACT

The AUC values of HIF-1α, TWIST-1, ITGB-1, and Ki-67 for predicting NACT responses and the optimal threshold required are summarized in Table 4. HIF-1α, TWIST-1, ITGB-1, and Ki-67 showed good power for predicting a favorable response (AUC = 0.81, 0.85, 0.79, and 0.80, respectively) and resistance to NACT (AUC = 0.83, 0.86, 0.84, 0.85, respectively). Among the new predictors, TWIST-1 showed the highest predictive power with the largest AUC values for both a favorable response (AUC = 0.85) and resistance (AUC = 0.86).

Furthermore, Ki-67 (traditional predictor) and TWIST-1 (the best new predictor) were combined into a new predictor (predRCB), which was generated using a multivariable linear regression model (predRCB = 1.819 + 0.012 × TWIST-1 − 0.01 × Ki-67). Compared with other single predictors, predRCB showed a better performance for predicting both a favorable response (AUC = 0.88) and resistance (AUC = 0.92) (Figure 4).

In addition, the results of AUC analysis of the predictive performance of predRCB among the different subgroups are shown in Table 5. PredRCB showed good accuracy (AUC > 0.80) in predicting NACT responses in the different subgroups, especially in patients with luminal A type, invasive lobular carcinoma, Grade 3, T3 tumor size, and TEC in NACT regimens.

Discussion

The results of this study can be summarized as follows: (i) Higher tumor stiffness was strongly correlated with higher
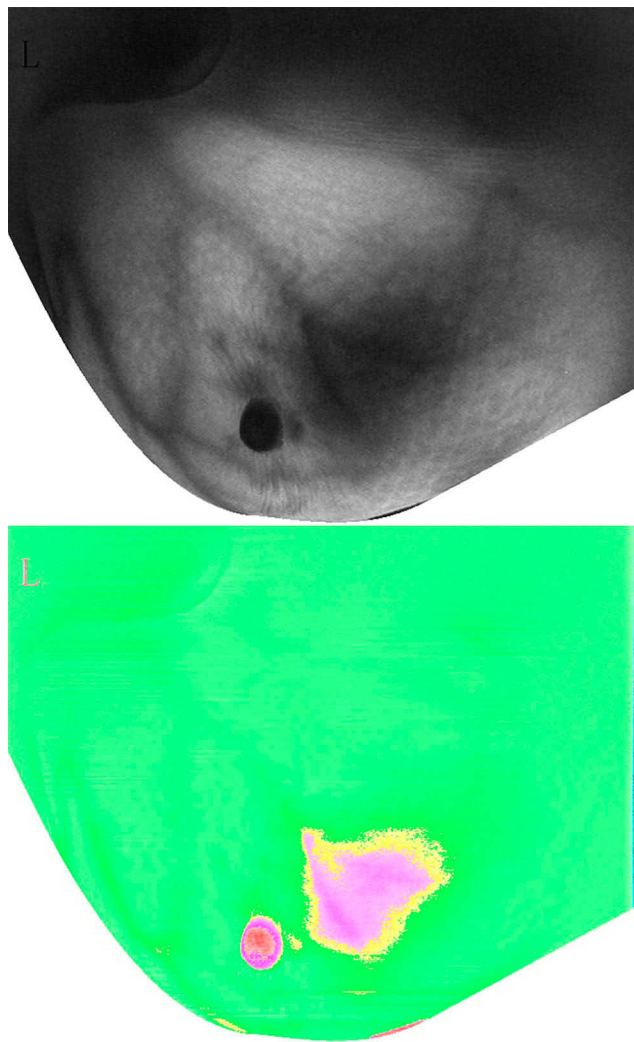
Figure 2 DOBI image with a ROI placed over the center point of the lesion with the OS values being automatically calculated by the system.
Abbreviations: DOBI, dynamic optical breast imaging; OS, oxygen score; ROI, region of interest.

HIF-1α, TWIST-1, and ITGB-1 expression and lower OS. (ii) HIF-1α, TWIST-1, ITGB-1, and Ki-67 expression exhibited good diagnostic performances for predicting a favorable response and resistance to NACT. (iii) PredRCB had considerably better power than HIF-1α, TWIST-1, ITGB-1, and Ki-67 alone for predicting NACT responses.

BC with higher stiffness evaluated by ultrasound elastography is closely correlated with chemoresistance.[9,29,30] Indeed, BC progression, invasion, and resistance to chemotherapeutic drugs are not only determined by the tumor cells themselves, but also by the extracellular microenvironment.[31] Basic research studies have confirmed that the cross-linking collagen in the ECM plays an important role in tissue stiffness.[32] However, the reason

why tumors with high stiffness tend to be resistant to NACT in BC remains unknown.

The two particularly important molecules of the ECM, collagen and hyaluronan (HA), participate in matrix stiffness, especially in the targeting of mechanotransduction in cancer.[30,33] Specifically, abnormal collagen composition or increased HA concentration can increase colloidal osmotic pressure, which can increase interstitial fluid pressure (IFP). High IFP can cause collapse of tumor vessels, thereby reducing microvascular perfusion and eventually limiting the delivery of chemotherapeutic drugs.[34,35]

Hypoxia is another extracellular microenvironment factor that plays an important role in regulating BC progression, invasion, metastasis, and chemotherapeutic resistance.[36,37] Zhu et al[37] analyzed the concentrations of total hemoglobin (t-Hb), oxygenated (oxy-Hb), and deoxygenated hemoglobin (deoxy-Hb) before chemotherapy by ultrasound-guided near-infrared optical tomography, and determined their association with pathologic responses to chemotherapy in 34 BC cases. The results indicated that hypoxia in BC tissues was strongly correlated with chemoresistance. In this study, we confirmed that invasive BC with lower stiffness and higher OS showed better NACT responses (PCR or RCBI), whereas tumors with higher stiffness and lower OS were associated with NACT resistance (RCBIII). These results are consistent with those of previous studies.[9,29,30,37]

This study is the first to use non-invasive imaging modalities to confirm the significant negative correlation between tumor stiffness and OS. The results can be explained as follows. (i) Matrix stiffness and neovascularization increase simultaneously during BC progression. However, the growth of vasculature in the tumor region does not meet the increased need for oxygen and nutrients in the neoplasm. An imbalance between blood oxygen demand and supply leads to hypoxia in tumor tissues. (ii) Increased matrix stiffness increases IFP, which causes tumor vascular collapse and compression. This further increases blood flow resistance, which reduces tumor microvascular blood perfusion, consumption of oxygen, and accumulation of waste, eventually leading to the formation of a hypoxic environment.

We hypothesized that increased matrix stiffness causes insufficient blood perfusion, which not only reduces drug delivery, but also induces hypoxia. The response to
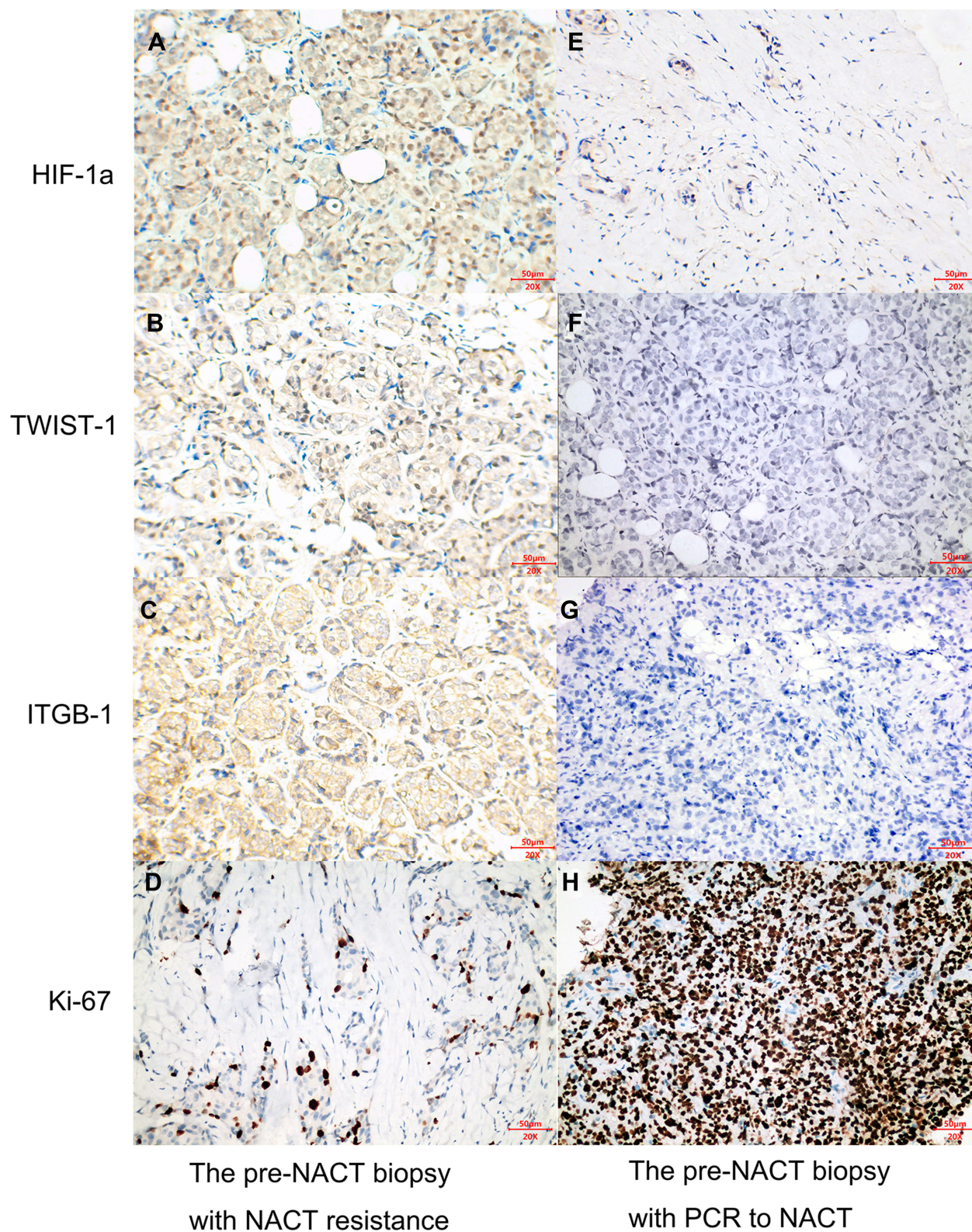
The pre-NACT biopsy
with NACT resistance

The pre-NACT biopsy
with PCR to NACT

Figure 3 Left column (**A–D**) Immunohistochemical analysis of a pre-NACT biopsy specimen from a patient with chemotherapy resistance. (**A**) High HIF-1α expression with a H score of 180; (**B**) high TWIST-1 expression with a H score of 160; (**C**) high ITGB-1 expression with a H score of 190; (**D**) low Ki-67 expression with a H score of 30. Right column (**E–H**) Immunohistochemical analysis of a pre-NACT biopsy specimen from a patient with PCR to NACT. (**E**) Low HIF-1α expression with a H score of 40; (**F**) low TWIST-1 expression with a H score of 6; (**G**) low ITGB-1 expression with a H score of 2; (**H**) High Ki-67 expression with a H score of 270.
Abbreviations: HIF-1α, hypoxia-inducible factor 1-alpha; ITGB-1, β1 integrin; NACT, neoadjuvant chemotherapy; PCR, pathological complete response; TWIST-1, twist family BHLH transcription factor 1.

Table 2 HIF-1α, TWIST1, ITGB1, and Ki-67 Expression in the Three RCB Groups

Biomarkers (H Score)	Total	PCR+RCB-I	RCB-II	RCB-III	P value
HIF-1α	115.61±56.7	73.9±34.1	103.7±42.3	161.8±57.0	<0.001 ¥,a,b,c
TWIST-1	83.0 (58.5–149.0)	57.7±23.5	88.4±38.3	154.2±62.2	<0.001 ¥,a,b,c
ITGB-1	100.3±54.8	64.3±37.7	87.0±37.0	144.8±58.8	<0.001 ¥,a,b,c
Ki-67	67.6±46.1	112.7±62.7	67.4±29.8	36.6±19.5	<0.001 ¥,a,b,c

Notes: ¥ANOVA test; [a]significant difference for pairwise comparison between PCR+RCBI and RCBII; [b]significant difference for pairwise comparison between PCR+RCBI and RCBIII; [c]significant difference for pairwise comparison between RCBII and RCBIII.
Abbreviations: PCR, pathological complete response; RCB, residual cancer burden; HIF-1α, hypoxia-inducible factor 1-alpha; TWIST-1, twist family BHLH transcription factor 1; ITGB-1, β1 integrin.

Table 3 Relationships Between HIF-1α, TWIST-1, ITGB-1, and Ki-67 Expression and SWE Stiffness and OS

Parameters	HIF-1α	TWIST-1	ITGB-1	Ki-67
Emax	0.708 (<0.001)*	0.621 (<0.001)	0.665 (<0.001)*	−0.244 (0.018)*
Emean	0.655 (<0.001)*	0.580 (<0.001)	0.637 (<0.001)*	−0.198 (0.044)*
OS	−0.644 (<0.001)	−0.622 (<0.001)	−0.618 (<0.001)	0.322 (0.001)

Notes: *Pearson's correlation analysis; Spearman's correlation analysis for remaining data.
Abbreviations: HIF-1α, hypoxia-inducible factor 1-alpha; TWIST-1, twist family BHLH transcription factor 1; ITGB-1, β1 integrin; Emax, maximum elasticity; Emean, mean elasticity; OS, oxygen score.

hypoxia is mainly regulated by HIF-1α in tumors, and HIF-1α is involved in tumorigenesis, growth, and metastasis in BC.[38,39] Furthermore, HIF-1α directly binds to and upregulates the expression of TWIST-1.[18,19,40] In addition, increased matrix stiffness activates and upregulates the expression of TWIST-1 in BC.[12] However, the mechanism by which TWIST-1 promotes BC resistance to NACT still needs to be elucidated. Recently, Yang et al[41] revealed that ECM–receptor interaction and the MAPK, PI3K/AKT, P53, and WNT signaling pathways are aberrantly activated in MCF10A-TWIST-1 cells based on iTRAQ-labeling combined with 2D LC-MS/MS analysis. These authors used ingenuity pathway analysis to show that TWIST-1 regulates these downstream proteins through ITGB-1. Thus, TWIST-1/ITGB-1 seems to be the upstream signaling molecules that induce invasion and metastasis in BC. In addition, over-expression of both TWIST-1 and ITGB-1 is associated with increased tumorigenesis, growth, metastasis, and resistance to chemotherapy in several cancers.[42,43]

Based on the analysis above, we propose a hypothesis to explain why high tumor stiffness is closely correlated with chemoresistance in BC. The IFP increases in tumor environments with high matrix stiffness, leading to heterogeneity and tortuosity of neovascularization. This leads to increased blood flow resistance, which reduces blood perfusion and increases

oxygen consumption. Finally, a hypoxic environment is formed in BC cells. The HIF-1α/TWIST-1/ITGB-1 pathway is activated, which causes BC phenotypic changes (eg, increased efflux of chemotherapeutic drugs, increased cytoprotective autophagy, and reduced apoptosis) through different downstream signaling pathways. These factors lead to the development of resistance to chemotherapeutic drugs. This study is the first to show that the expression levels of HIF-1α, TWIST-1, and ITGB-1 are positively correlated with stiffness and negatively correlated with OS in BC patients. In addition, we found a direct association among the expression levels of HIF-1α, TWIST-1, and ITGB-1. Moreover, higher expression levels of HIF-1α, TWIST-1, and ITGB-1 were inter-related in the NACT resistance group (RCBIII). These results strongly support the hypothesis above. However, the mechanism underlying the function of the HIF-1α/TWIST-1/ITGB-1 axis and downstream signaling needs to be investigated in further prospective studies in vitro and in vivo.

We also used these biomarkers to predict the pathological response to NACT in BC. The results demonstrated that HIF-1α, TWIST-1, and ITGB-1 show comparable abilities for the accurate assessment and prediction of NACT responses. To the best of our knowledge, this is the first study to report the performance of HIF-1α, TWIST-1, and ITGB-1 for predicting

Table 4 Predictive Diagnostic Performance of HIF-1α, TWIST-1, ITGB-1, Ki-67, and PredRCB for Predicting Responses to NACT

Predictor	Favourable Response							Resistant Response						
	AUC	SE	95% CI	P value	Cut-off*	Sensitivity (%)	Specificity (%)	AUC	SE	95% CI	P value	Cut-off*	Sensitivity (%)	Specificity (%)
New														
HIF-1α	0.81	0.049	0.71–0.90	<0.001	≤71.0	84.0	65.2	0.83	0.042	0.75–0.91	<0.001	>107.0	87.9	73.8
TWIST-1	0.85	0.042	0.77–0.93	<0.001	≤66.0	77.8	78.3	0.86	0.037	0.79–0.94	<0.001	>112.0	81.8	81.7
ITGB-1	0.79	0.057	0.67–0.90	<0.001	≤57.0	86.4	65.2	0.84	0.042	0.75–0.92	<0.001	>93.0	84.8	71.8
Traditional														
Ki-67	0.80	0.049	0.71–0.90	<0.001	≥49.0	95.7	51.9	0.85	0.039	0.77–0.92	<0.001	<49.0	77.5	81.8
Combined														
PredRCB	0.88	0.034	0.82–0.95	<0.001	≤2.075	72.8	95.7	0.92	0.027	0.86–0.97	<0.001	>2.717	81.8	87.3

Note: *Cut-offs were generated by the best Youden index.
Abbreviations: HIF-1α, hypoxia-inducible factor 1-alpha; TWIST-1, twist family BHLH transcription factor 1; ITGB-1, β1 integrin; AUC, area under the receiver operating characteristic curve; SE, standard error; CI, confidence interval.

the response to NACT in BC. Ki-67 is a biological marker associated with cell proliferation and is regarded as the traditional marker for predicting the response to NACT in BC.[6] In this study, Ki-67 also showed a good predictive performance. These results strongly support previous findings.[6,44]

This study also showed that a combination of pathological markers can improve the power of single markers for predicting the response to NACT in BC. TWIST-1 and Ki-67, which showed the best performance for predicting different responses, were combined into a new predictive marker termed predRCB using a linear regression model. The results showed that the performance of predRCB was better than that of the other biomarkers alone for predicting NACT responses. In the subgroup analysis, we confirmed that the predictive power of predRCB was not influenced by tumor classification, subtype, or NACT regimens. This provided strong evidence that our conclusions had generalizability and validity.

Clinically, identifying a method to reverse or block chemoresistance in BC with high tissue stiffness is important. In in vitro cultures mimicking stiffness changes during BC progression, alterations in ECM rigidity might aberrantly activate certain mechanotransduction pathways, resulting in various tumorigenic processes, such as sustained proliferation, EMT, invasion, metastasis, and resistance to cell death.[31,45-47] However, alterations in ECM rigidity cannot be induced in the human body because cells normally exist in a physiologic environment with specific rigidity, pressure, and strain. Several studies have investigated whether markers such as HIF-1α, TWIST-1, and ITGB-1 can be used as therapeutic targets to reverse or block resistance to chemotherapy in BC. Some of the results are as follows. (i) HIF-1α: HIF-1α inhibitors such as digoxin and acriflavine show convincing potential therapeutic effects by decreasing tumor growth, vascularization, invasion, and metastasis, as well as chemoresistance in animal models of BC.[48,49] (ii) TWIST-1: TWIST-1 is an excellent target for modulating chemoresistance in BC because it is rarely expressed in normal human tissues.[50] Therefore, systemic use of TWIST-1 inhibitors could have a significant effect on TWIST-1-overexpressing cancer cells with minimal side effects in other tissues. The inactivation of TWIST-1 by siRNA technology or chemotherapeutic approaches was shown to be successful,[51–53] and several inhibitors have been identified to antagonize the upstream or
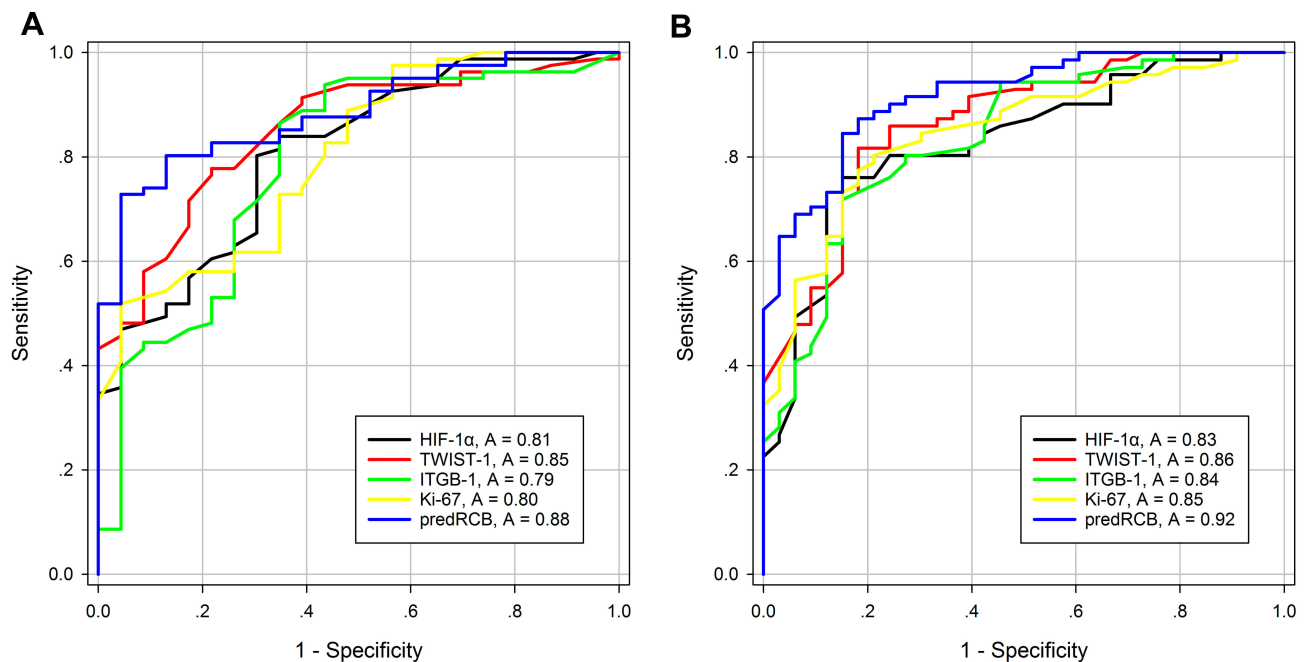
Figure 4 ROC curves of HIF-1α, TWIST-1, ITGB-1, Ki-67 index and predRCB for predicting (**A**) a favorable response to NACT and (**B**) resistance to NACT.
Abbreviations: HIF-1α, hypoxia-inducible factor 1-alpha; ITGB-1, β1 integrin; TWIST-1, twist family BHLH transcription factor 1; RCB, residual cancer burden; ROC, receiver operating characteristic.

downstream molecules of TWIST signaling.[54] Recently, cancer stem cell-targeted nanoparticle delivery has received increased attention. Finlay et al[55] verified the in vivo efficacy of mesoporous silica nanoparticle (MSN)-delivered siRNA in a mouse model of melanoma. Similar data were reported in ovarian cancer, where the tumor burden was significantly reduced by 75% in mice treated with siTWIST MSN plus chemotherapy compared with the control chemotherapy-only treated mice.[56] (iii) ITGB-1: Increasing evidence suggests that ITGB-1 is a potential molecular therapeutic target in BC.[57,58] The therapeutic potential of targeting ITGB-1 using various strategies or inhibitors, such as monoclonal antibodies, peptides, or synthetic peptides, and siRNA is being investigated. Inhibitors that silence ITGB-1 were shown to suppress tumor progression and metastasis in vitro and in vivo.

However, most of these studies are based on basic experiments. Further clinical trials are warranted to determine whether HIF-1α/TWIST-1/ITGB-1 targeting strategies can reverse or block the chemotherapeutic resistance of BC alone or in combination with current therapeutic regimens.

The present study had several limitations. First, the study was based on a relatively small sample size.

Second, the endogenous expression of HIF-1α, TWIST-1, ITGB-1, and Ki-67 in the tumor (as a three-dimensional structure) showed an uneven distribution. The expression of HIF-1α, TWIST-1, ITGB-1, and Ki-67 was assessed using tissues obtained by CNB. However, local samples obtained by CNB do not fully reflect the heterogeneity of the entire tumor. Taking the average of multi-site biopsies might reduce this difference. Finally, disease-free survival and overall survival analyses could not be performed because of the short follow-up period. A prospective study with a longer follow-up period should be conducted to confirm the present results.

Conclusion

First, higher HIF-1α, TWIST-1, and ITGB-1 expression levels were strongly correlated with higher tumor stiffness and lower OS in BC patients. Second, HIF-1α, TWIST-1, and ITGB-1 expression exhibited a good diagnostic performance for the early prediction of NACT responses in BC. Third, this study highlighted the potential utility of predRCB, which could improve the diagnostic performance of single markers for the early prediction of different pathological responses and

Table 5 Performance of predRCB for Predicting Responses to NACT in the Different Subgroups

Subtype	Favourable Response				Resistant Response			
	AUC	SE	95% CI	*P* value	AUC	SE	95% CI	*P* value
Molecular subtype								
Luminal A	1.00	0.000	1.00–1.00	0.005	0.93	0.07	0.79–1.00	0.01
Luminal B	0.90	0.044	0.81–0.98	<0.001	0.91	0.04	0.83–0.99	<0.001
Triple negative	0.89	0.101	0.69–1.00	0.010	–	–	–	–
HER2	0.95	0.05	0.85–1.00	0.003	0.78	0.17	0.44–1.00	0.20
Pathological types								
Invasive ductal carcinoma	0.86	0.04	0.78–0.94	<0.001	0.92	0.03	0.86–0.97	<0.001
Invasive lobular carcinoma	1.00	0.00	1.00–1.00	0.014	0.95	0.07	0.81–1.00	0.03
Grade								
Grade 2	0.88	0.04	0.81–0.95	<0.001	0.90	0.03	0.84–0.97	<0.001
Grade 3	1.00	0.00	1.00–1.00	0.005	1.00	0.00	1.00–1.00	0.003
Tumor size (cT)								
T1	0.57	0.20	0.19–0.96	0.770	–	–	–	–
T2	0.84	0.05	0.75–0.94	<0.001	0.88	0.04	0.80–0.96	<0.001
T3	1.00	0.00	1.00–1.00	<0.001	0.96	0.03	0.90–1.00	<0.001
NACT regimens:								
TEC	0.93	0.03	0.86–1.00	<0.001	0.92	0.03	0.85–0.98	<0.001
TE	0.64	0.18	0.30–0.99	0.450	1.00	0.00	1.00–1.00	0.114
FEC	–	–	–	–	0.79	0.15	0.48–1.00	0.242
TH	0.75	0.11	0.54–0.96	0.261	1.00	0.00	1.00–1.00	0.008

Note: "–": Unable to calculate due to small sample size after subgrouping.
Abbreviations: NACT, neoadjuvant chemotherapy; TEC, (docetaxel, epirubicin, and cyclophosphamide); TE (docetaxel and epirubicin); FEC (5-fluorouracil, epirubicin, and cyclophosphamide); TH (docetaxel and herceptin); AUC, area under the receiver operating characteristic curve; SE, standard error. CI, confidence interval.

assist in clinical treatment decisions in patients with BC receiving NACT.

Abbreviations

AUC, area under the curve; BC, breast cancer; CNB, core needle biopsy; Deoxy-Hb, deoxygenated hemoglobin; DOBI, dynamic optical breast imaging; ECM, extracellular matrix; Emax, maximum elasticity; Emean, mean elasticity; FEC, 5-fluorouracil, epirubicin, and cyclophosphamide; HA, hyaluronan; HIF-1α, hypoxia-inducible factor 1-alpha; ITGB-1, β1 integrin; NACT, neoadjuvant chemotherapy; OS, oxygen score; Oxy-Hb, oxygenated hemoglobin; PCR, pathological complete response; RCB, residual cancer burden; ROC, receiver operating characteristic; ROI, region of interest; SWE, shear-wave elastography; T-Hb, total hemoglobin; TWIST-1, twist family BHLH transcription factor 1; TEC, docetaxel, epirubicin, and cyclophosphamide; TE, docetaxel and epirubicin; TH, docetaxel and herceptin; US, ultrasound.

Author Contributions

All authors contributed toward data analysis and drafting and revising the paper, and agree to be accountable for all aspects of the work.

Ethics and Consent Statement

The study was conducted with the approval of the Ethics Committee of Shengjing Hospital of China Medical University. All patients provided written informed consent. This study was conducted in accordance with the Declaration of Helsinki.

Disclosure

The authors report no conflicts of interest in this work.

References

1. Bartsch R, Bergen E, Galid A. Current concepts and future directions in neoadjuvant chemotherapy of breast cancer. *Memo*. 2018;11 (3):199–203. doi:10.1007/s12254-018-0421-1

2. Rubovszky G, Horváth Z. Recent advances in the neoadjuvant treatment of breast cancer. *J Breast Cancer*. 2017;20(2):119–131. doi:10.4048/jbc.2017.20.2.119

3. Crippa F, Agresti R, Sandri M, et al. 18F-FLT PET/CT as an imaging tool for early prediction of pathological response in patients with locally advanced breast cancer treated with neoadjuvant chemotherapy: a pilot study. *Eur J Nucl Med Mol Imaging*. 2015;42 (6):818–830. doi:10.1007/s00259-015-2995-8

4. Chen S, Huang L, Chen CM, Shao ZM. Progesterone receptor loss identifies luminal-type local advanced breast cancer with poor survival in patients who fail to achieve a pathological complete response to neoadjuvant chemotherapy. *Oncotarget*. 2015;6(20):18174–18182. doi:10.18632/oncotarget.4225

5. Dai Z, Wang X, Li Z, et al. HER-2 expression in local advanced breast cancer and the efficacy of neoadjuvant chemotherapy regimens. *Nan Fang Yi Ke Da Xue Xue Bao*. 2007;27(9):1397–1399.

6. Jain P, Doval D, Batra U, et al. Ki-67 labeling index as a predictor of response to neoadjuvant chemotherapy in breast cancer. *Jpn J Clin Oncol*. 2019;49(4):329–338. doi:10.1093/jjco/hyz012

7. Bownes RJ, Turnbull AK, Martinez-Perez C, Cameron DA, Sims AH, Oikonomidou O. On-treatment biomarkers can improve prediction of response to neoadjuvant chemotherapy in breast cancer. *Breast Cancer Res*. 2019;21(1):73. doi:10.1186/s13058-019-1159-3

8. Park KU, Chen Y, Chitale D, et al. Utilization of the 21-gene recurrence score in a diverse breast cancer patient population: development of a clinicopathologic model to predict high-risk scores and response to neoadjuvant chemotherapy. *Ann Surg Oncol*. 2018;25 (7):1921–1927. doi:10.1245/s10434-018-6440-7

9. Ma Y, Zhang S, Li J, Li J, Kang Y, Ren W. Comparison of strain and shear-wave ultrasonic elastography in predicting the pathological response to neoadjuvant chemotherapy in breast cancers. *Eur Radiol*. 2016;27(6):2282–2291. doi:10.1007/s00330-016-4619-5

10. Ma Y, Zhang S, Zang L, et al. Combination of shear wave elastography and Ki-67 index as a novel predictive modality for the pathological response to neoadjuvant chemotherapy in patients with invasive breast cancer. *Eur J Cancer*. 2016;69:86–101. doi:10.1016/j.ejca.2016.09.031

11. Giussani M, Merlino G, Cappelletti V, Tagliabue E, Daidone MG. Tumor-extracellular matrix interactions: identification of tools associated with breast cancer progression. *Semin Cancer Biol*. 2015;35:3–10. doi:10.1016/j.semcancer.2015.09.012

12. Wei SC, Fattet L, Tsai JH, et al. Matrix stiffness drives epithelial–mesenchymal transition and tumour metastasis through a TWIST1–G3BP2 mechanotransduction pathway. *Nat Cell Biol*. 2015;17 (5):678–688. doi:10.1038/ncb3157

13. Ondeck M, Kumar A, Placone J, et al. Dynamically stiffened matrix promotes malignant transformation of mammary epithelial cells via collective mechanical signaling. *Proc Natl Acad Sci USA*. 2019;116 (9):3502–3507. doi:10.1073/pnas.1814204116

14. Glackin AC. Targeting the Twist and Wnt signaling pathways in metastatic breast cancer. *Maturitas*. 2014;79(1):48–51. doi:10.1016/j.maturitas.2014.06.015

15. Glackin C. Nanoparticle delivery of TWIST small interfering RNA and anticancer drugs: a therapeutic approach for combating cancer. *Enzymes*. 2018;44:83–101.

16. Gilkes DM, Bajpai S, Chaturvedi P, Wirtz D, Semenza GL. Hypoxia-inducible factor 1 (HIF-1) promotes extracellular matrix remodeling under hypoxic conditions by inducing P4HA1, P4HA2, and PLOD2 expression in fibroblasts. *J Biol Chem*. 2013;288(15):10819–10829. doi:10.1074/jbc.M112.442939

17. Semenza GL. Hypoxia-inducible factors: mediators of cancer progression and targets for cancer therapy. *Trends Pharmacol Sci*. 2012;33(4):207–214. doi:10.1016/j.tips.2012.01.005

18. Yang MH, Wu K-J. TWIST activation by hypoxia inducible factor-1 (HIF-1): implications in metastasis and development. *Cell Cycle*. 2008;7(14):2090–2096. doi:10.4161/cc.7.14.6324

19. Liu Y, Huang X, Yu H, et al. HIF-1α-TWIST pathway restrains cyclic mechanical stretch-induced osteogenic differentiation of bone marrow mesenchymal stem cells. *Connect Tissue Res*. 2019;60 (6):544–554. doi:10.1080/03008207.2019.1601185

20. Barnawi R, Al-Khaldi S, Colak D, et al. β1 Integrin is essential for fascin-mediated breast cancer stem cell function and disease progression. *Int J Cancer*. 2019;145(3):830–841. doi:10.1002/ijc.32183

21. Yuan J, Liu M, Yang L, et al. Acquisition of epithelial-mesenchymal transition phenotype in the tamoxifen-resistant breast cancer cell: a new role for G protein-coupled estrogen receptor in mediating tamoxifen resistance through cancer-associated fibroblast-derived fibronectin and β1-integrin signaling pathway in tumor cells. *Breast Cancer Res*. 2015;17:69.

22. Olivares-Navarrete R, Lee EM, Smith K, et al. Substrate stiffness controls osteoblastic and chondrocytic differentiation of mesenchymal stem cells without exogenous stimuli. *PLoS One*. 2017;12(1): e0170312. doi:10.1371/journal.pone.0170312

23. D'Aiuto M, Frasci G, Barretta ML, et al. The dynamic optical breast imaging in the preoperative workflow of women with suspicious or malignant breast lesions: development of a new comprehensive score. *ISRN Oncol*. 2012;2012(2012):631917.

24. Wolff AC, Hammond MEH, Allison KH, et al. Human epidermal growth factor receptor 2 testing in breast cancer: American Society of Clinical Oncology/College of American Pathologists Clinical Practice Guideline Focused Update. *J Clin Oncol*. 2018;36 (20):2105–2122. doi:10.1200/JCO.2018.77.8738

25. Wu L, Yi B, Wei S, et al. Loss of FOXP3 and TSC1 accelerates prostate cancer progression through synergistic transcriptional and posttranslational regulation of c-MYC. *Cancer Res*. 2019;79 (7):1413–1425. doi:10.1158/0008-5472.CAN-18-2049

26. Goldhirsch A, Winer EP, Coates AS, et al. Personalizing the treatment of women with early breast cancer: highlights of the St Gallen international expert consensus on the primary therapy of early breast cancer 2013. *Ann Oncol*. 2013;24(9):2206–2223. doi:10.1093/annonc/mdt303

27. Symmans WF, Peintinger F, Hatzis C, et al. Measurement of residual breast cancer burden to predict survival after neoadjuvant chemotherapy. *J Clin Oncol*. 2007;25(28):4414–4422. doi:10.1200/JCO.2007.10.6823

28. Koo TK, Li MY. A guideline of selecting and reporting intraclass correlation coefficients for reliability research. *J Chiropr Med*. 2016;15(2):155–163. doi:10.1016/j.jcm.2016.02.012

29. Fernandes J, Sannachi L, Tran W, et al. Monitoring breast cancer response to neoadjuvant chemotherapy using ultrasound strain elastography. *Transl Oncol*. 2019;12(9):1177–1184. doi:10.1016/j.tranon.2019.05.004

30. Katyan A, Mittal M, Mani C, Mandal A. Strain wave elastography in response assessment to neo-adjuvant chemotherapy in patients with locally advanced breast cancer. *Br J Radiol*. 2019;92 (1099):20180515. doi:10.1259/bjr.20180515

31. Majeski HE, Yang J. The 2016 John J. Abel award lecture: targeting the mechanical microenvironment in cancer. *Mol Pharmacol*. 2016;90(6):744–754. doi:10.1124/mol.116.106765

32. Humphrey JD, Dufresne ER, Schwartz MA. Mechanotransduction and extracellular matrix homeostasis. *Nat Rev Mol Cell Biol*. 2014;15(12):802–812. doi:10.1038/nrm3896

33. Cox TR, Bird D, Baker A-M, et al. LOX-mediated collagen cross-linking is responsible for fibrosis-enhanced metastasis. *Cancer Res*. 2013;73(6):1721–1732. doi:10.1158/0008-5472.CAN-12-2233

34. Provenzano P, Cuevas C, Chang A, Goel V, Von Hoff D, Hingorani S. Enzymatic targeting of the stroma ablates physical barriers to treatment of pancreatic ductal adenocarcinoma. *Cancer Cell*. 2012;21 (3):418–429. doi:10.1016/j.ccr.2012.01.007

35. Jacobetz MA, Chan DS, Neesse A, et al. Hyaluronan impairs vascular function and drug delivery in a mouse model of pancreatic cancer. *Gut*. 2013;62(1):112–120. doi:10.1136/gutjnl-2012-302529

36. Gao T, Li J-Z, Lu Y, et al. The mechanism between epithelial mesenchymal transition in breast cancer and hypoxia microenvironment. *Biomed Pharmacother*. 2016;80:393–405. doi:10.1016/j.biopha.2016.02.044

37. Zhu Q, Wang L, Tannenbaum S, Ricci A, DeFusco P, Hegde P. Pathologic response prediction to neoadjuvant chemotherapy utilizing pretreatment near-infrared imaging parameters and tumor pathologic criteria. *Breast Cancer Res*. 2014;16(5):456. doi:10.1186/s13058-014-0456-0

38. Kozlova N, Wottawa M, Katschinski DM, Kristiansen G, Kietzmann T. Hypoxia-inducible factor prolyl hydroxylase 2 (PHD2) is a direct regulator of epidermal growth factor receptor (EGFR) signaling in breast cancer. *Oncotarget*. 2017;8(6):9885–9898. doi:10.18632/oncotarget.v8i6

39. Mukund V, Saddala M, Farran B, Mannavarapu M, Alam A, Nagaraju G. Molecular docking studies of angiogenesis target protein HIF-1α and genistein in breast cancer. *Gene*. 2019;701:169–172. doi:10.1016/j.gene.2019.03.062

40. Saponaro C, Vagheggini A, Scarpi E, et al. NHERF1 and tumor microenvironment: a new scene in invasive breast carcinoma. *J Exp Clin Cancer Res*. 2018;37(1):96. doi:10.1186/s13046-018-0766-7

41. Yang J, Hou Y, Zhou M, et al. Twist induces epithelial-mesenchymal transition and cell motility in breast cancer via ITGB1-FAK/ILK signaling axis and its associated downstream network. *Int J Biochem Cell Biol*. 2016;71:62–71. doi:10.1016/j.biocel.2015.12.004

42. Liu Y, Yin P, Silvers C, Lee Y. Enhanced metastatic potential in the MB49 urothelial carcinoma model. *Sci Rep*. 2019;9(1):7425. doi:10.1038/s41598-019-43641-5

43. Xu ZY, Chen J-S, Shu Y-Q. Gene expression profile towards the prediction of patient survival of gastric cancer. *Biomed Pharmacother*. 2010;64(2):133–139. doi:10.1016/j.biopha.2009.06.021

44. Kim KI, Lee KH, Kim TR, Chun YS, Lee TH, Park HK. Ki-67 as a predictor of response to neoadjuvant chemotherapy in breast cancer patients. *J Breast Cancer*. 2014;17(1):40–46. doi:10.4048/jbc.2014.17.1.40

45. Levental KR, Yu H, Kass L, et al. Matrix crosslinking forces tumor progression by enhancing integrin signaling. *Cell*. 2009;139 (5):891–906. doi:10.1016/j.cell.2009.10.027

46. Leight JL, Wozniak MA, Chen S, Lynch ML, Chen CS. Matrix rigidity regulates a switch between TGF-β1-induced apoptosis and epithelial-mesenchymal transition. *Mol Biol Cell*. 2012;23(5):781–791. doi:10.1091/mbc.e11-06-0537

47. Paszek M, DuFort C, Rossier O, et al. The cancer glycocalyx mechanically primes integrin-mediated growth and survival. *Nature*. 2014;511(7509):319–325. doi:10.1038/nature13535

48. Wong CC, Zhang H, Gilkes DM, et al. Inhibitors of hypoxia-inducible factor 1 block breast cancer metastatic niche formation and lung metastasis. *J Mol Med (Berl)*. 2012;90(7):803–815. doi:10.1007/s00109-011-0855-y

49. Schito L, Rey S, Tafani M, et al. Hypoxia-inducible factor 1-dependent expression of platelet-derived growth factor B promotes lymphatic metastasis of hypoxic breast cancer cells. *Proc Natl Acad Sci USA*. 2012;109(40):E2707–E2716. doi:10.1073/pnas.1214019109

50. Qin Q, Xu Y, He T, Qin C, Xu J. Normal and disease-related biological functions of Twist1 and underlying molecular mechanisms. *Cell Res*. 2012;22(1):90–106. doi:10.1038/cr.2011.144

51. Wang WS, Yang XS, Xia M, Jiang HY, Hou JQ. Silencing of twist expression by RNA interference suppresses epithelial-mesenchymal transition, invasion, and metastasis of ovarian cancer. *Asian Pac J Cancer Prev*. 2012;13(9):4435–4439. doi:10.7314/APJCP.2012.13.9.4435

52. Fan C, Prat A, Parker JS, et al. Building prognostic models for breast cancer patients using clinical variables and hundreds of gene expression signatures. *BMC Med Genomics*. 2011;4(1):3. doi:10.1186/1755-8794-4-3

53. Ma G, He J, Yu Y, et al. Tamoxifen inhibits ER-negative breast cancer cell invasion and metastasis by accelerating Twist1 degradation. *Int J Biol Sci*. 2015;11(5):618–628. doi:10.7150/ijbs.11380

54. Shi J, Cao J, Zhou BP. Twist-BRD4 complex: potential drug target for basal-like breast cancer. *Curr Pharm Des*. 2015;21(10):1256–1261. doi:10.2174/1381612821666141211153853

55. Finlay J, Roberts CM, Dong J, Zink JI, Tamanoi F, Glackin CA. Mesoporous silica nanoparticle delivery of chemically modified siRNA against TWIST1 leads to reduced tumor burden. *Nanomed*. 2015;11(7):1657–1666. doi:10.1016/j.nano.2015.05.011

56. Roberts CM, Shahin SA, Wen W, et al. Nanoparticle delivery of siRNA against TWIST to reduce drug resistance and tumor growth in ovarian cancer models. *Nanomed*. 2017;13(3):965–976. doi:10.1016/j.nano.2016.11.010

57. Klahan S, Huang WC, Chang CM, et al. Gene expression profiling combined with functional analysis identify integrin beta1 (ITGB1) as a potential prognosis biomarker in triple negative breast cancer. *Pharmacol Res*. 2015;104:31–37. doi:10.1016/j.phrs.2015.12.004

58. Blandin AF, Renner G, Lehmann M, Lelong-Rebel I, Martin S, Dontenwill M. β1 integrins as therapeutic targets to disrupt hallmarks of cancer. *Front Pharmacol*. 2015;6:279. doi:10.3389/fphar.2015.00279